

# Prediction of brittle-to-ductile transitions in polystyrene

H.G.H. van Melick, L.E. Govaert\*, H.E.H. Meijer

*Dutch Polymer Institute (DPI), Section Materials Technology (MaTe), Eindhoven University of Technology,  
P.O. Box 513, NL-5600MB Eindhoven, The Netherlands*

## Abstract

In this study it is attempted to predict brittle-to-ductile transitions (BDTs) in polystyrene blends, induced either by an increase in temperature or by a decrease in inter-particle distance. A representative, two-dimensional volume element (RVE) of a polystyrene matrix with 20% circular voids, is deformed in tension. During deformation a hydrostatic-stress based craze-nucleation criterion [1] is evaluated. The simulations demonstrate that crazes initiate at low temperatures while a transition from crazing to shear yielding (BDT) is found around 75 °C. The numerical results correlate well with tensile tests on similar heterogeneous polystyrene. The presence of an absolute length, as experimentally found, is more difficult to explain. Near a free surface a  $T_g$ -depression is measured for polystyrene and also the resistance to indentation in polystyrene is lower than expected from bulk properties. Both observations are rationalised by an enhanced segmental mobility of chains near a free surface. As a consequence of these findings, an absolute length-scale could be incorporated in the numerical simulations. For simplicity, the length-scale is modelled by taking a temperature gradient over a thin layer near the internal free surfaces of the RVE. Deformation of the RVE with different absolute length-scales shows that indeed also the experimentally found brittle-to-ductile transition can be predicted if the ligament thickness between the inclusions ('voids') in polystyrene is below a critical value of ca. 15 nm.

© 2002 Elsevier Science Ltd. All rights reserved.

**Keywords:** Brittle-to-ductile transition; Polystyrene; Finite element simulations

## 1. Introduction

Numerical prediction of strain localisation phenomena in glassy polymers has received substantial attention during the last decades. Following the work of Haward and Thackray [2], Boyce and co-workers [3–6] developed a model that was able to capture the post-yield behaviour of glassy polymers. Studies of the group of van der Giessen [7, 8] and our group [9–17] lead to the conclusion that the numerical simulation of plastic localisation in various loading geometries is now well established. However, failure, an important issue in the deformation behaviour, could not yet be predicted.

The importance of failure prediction can be envisaged by taking the macroscopic deformation behaviour of polystyrene as an example. Already in the apparent elastic region crack-like defects, so-called *crazes*, appear at the surface of a tensile bar under loading. The faces of these crazes are bridged by fibrillar material, which provides the crazes some load bearing capacity. From the highly stretched fibrils [18,19] it can be witnessed that on a local

scale polystyrene is extremely ductile, but, due to its pronounced strain softening and weak strain hardening, the strain tends to localise in these small local zones that cannot be stabilised [20].

Kramer [21] recognised that the extreme localisation is even to be considered as a prerequisite event for the initiation of the crazes. His main conclusion was that the formation of a small, localised plastic deformation zone, within a relatively undeformed matrix, first leads to a build-up of tri-axial stresses. Subsequently, this deformation can either be stabilised provided that the polymer network is able to transfer sufficient load, or cannot be stabilised causing the localisation to evolve to extremes meanwhile building-up dilative stresses until, at a sufficiently high dilative stress (successive), nucleation of voids occurs. With ongoing deformation the voids coalesce into a void network and form a craze.

Resistance to void nucleation is dependent on the network density of polymers [22–24]. This partly explains the craze- and defect-sensitivity of polystyrene that forms—due to its high chain stiffness—a low entangled network. Recently it was shown, by means of a combined experimental and numerical indentation study, that void nucleation, indeed preceded by plastic deformation, in

---

\* Corresponding author. Tel.: +31-40-2472838; fax: +31-40-2447355.  
E-mail address: l.e.govaert@tue.nl (L.E. Govaert).

polystyrene occurs at a critical hydrostatic stress of 40 MPa [1]. With increasing network density this critical hydrostatic stress level was found to increase.

The build-up of high dilative stresses, which ultimately leads to crazing, can only be circumvented by introducing heterogeneity into the material. For polystyrene, the incorporation of rubber particles resulted in a mechanism that is identified as *multiple crazing* [25–27]. Although this engineering method increased the material volume participating in the deformation process and, thus increased toughness, it did not lead to a transition from crazing to shear yielding and can, consequently, be considered to be only a partial solution to the problem. The ultimate toughness improvement should induce such a crazing to shear yielding transition. This can only be achieved by two routes. Either the overall stress level has to be lowered such that a critical stress level is not reached, or the thickness of the polymer ligaments in between the inclusions has to be reduced such that crazing cannot occur [28–31]. The first route proves to be not very practical, but indeed can be realised, e.g. by increasing the test temperature, by (mechanical) rejuvenation of the material, or by adding plasticisers. The latter route introduces the concept of a critical inter-particle thickness [31,32] and relies on the explanation that an absolute length-scale in the material is met. Recently, evidence is reported concerning the existence of this absolute length-scale. A reduced glass-transition temperature,  $T_g$ , was found for thin polystyrene films [33–35], rationalised by an enhanced mobility of chains near a free surface, and nano-indentation experiments showed a decreased resistance to indentation at shallow indentation depth (100 nm) near the free surface of bulk polystyrene [36]. In the present study the deformation of heterogeneous polystyrene systems is investigated by means of finite elements simulations, employing the compressible Leonov model [9,10]. A system of polystyrene with 20% voids is modelled as a representative volume element (RVE) [17]. During deformation, the stress and strain distributions are monitored and the critical hydrostatic stress criterion (40 MPa) for craze nucleation [1] is continuously evaluated. Since increasing the testing temperature results in an overall lowering of the stress level, the simulations are performed at various temperatures to identify a transition from crazing to shear yielding. The results of the predicted brittle-to-ductile transition are compared to the results of uni-axial tensile tests on polystyrene filled with 20% non-adhering core-shell rubbers.

Next the influence of an absolute length-scale is investigated in the simulations. The enhanced segmental mobility, held responsible for the  $T_g$ -decrease in thin polystyrene films, is modelled with a temperature gradient over a thin layer near free surfaces of the RVE. By varying the width of this gradient, the deformation of RVE with different length-scales is investigated, finally leading to an absolute length-scale dependent brittle-to-ductile transition that was earlier found in experiments.

## 2. Numerical modelling

The constitutive model, successfully used for glassy polymers, is the compressible Leonov model, extensively described in Refs. [9–11]. Validation of the model for polystyrene can be found in Ref. [20]. Finite element simulations of a RVE are used here to study the effect of the intrinsic properties on the macroscopic deformation behaviour and to, locally, evaluate stresses and strains in order to obtain a failure criterion. The RVE, a 2D representation of the micro-structure on the lowest level considered in multi-level FEM [13], is composed of a polymer matrix containing different volume fractions of randomly packed inclusions, in the simplest case consisting of spherical holes. The procedure to create such an RVE starts with the random filling of a unit box with the desired volume percentage (20% in this case) of mono-sized spheres with diameter equal to 5% of the dimension of the unit box. Next an arbitrary cross-section through this box is meshed with plain strain 8-node quadrilateral elements (reduced integration) using MENTAT (MSC Software). The use of these quadrilateral elements proved to be necessary in the combination of the material model used with the excessive deformation inside the heterogeneous structure. At least five elements spanning the width of every ligament were required to obtain a fair description of the (large) deformations within the ligaments. This large number of elements required within the ligaments limited the maximum size of the RVE, thereby obstructing the representative character of the RVE (to be completely independent of the initial—random—choice of the RVE, roughly 300 inclusions should have been modelled, see Ref. [14]). The finite element mesh is composed of 7256 plane-strain 8-node quadrilateral reduced integration elements, as shown in Fig. 1.

To prevent rigid body movement the lower-left node is fixed in  $x$ - and  $y$ -direction, whereas the top-left node is only fixed in  $x$ -direction. Furthermore periodic boundary

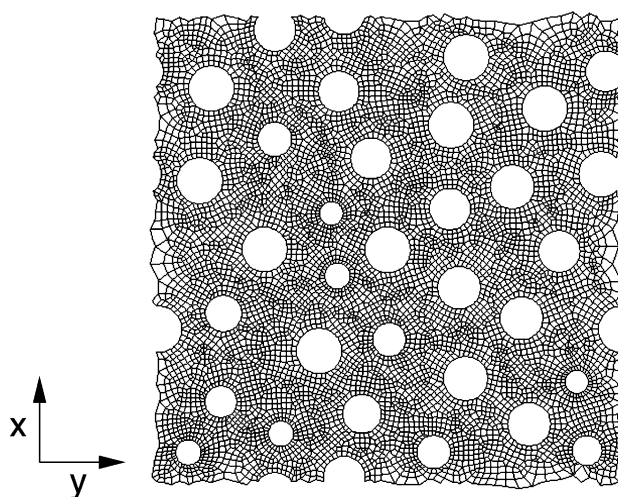


Fig. 1. FEM mesh of an RVE for finite element simulations.

conditions are assumed on the edges of the RVE. These ensure that the right-hand side and top always fit to, respectively, the left-hand side and bottom and the RVE can be regarded as a representative part of a whole structure. Since the compressible Leonov finite element formulation [37] is available for 2D simulations only, plane strain conditions are assumed. In all simulations, a linear macroscopic strain-rate of  $10^{-3} \text{ s}^{-1}$  is applied in  $x$ -direction to deform the RVE. The RVE is loaded up to a macroscopic strain of 20%, since beyond this strain local re-meshing proved to be required to obtain an adequate description of the deformation of the excessively deformed ligaments.

### 3. Numerical strategy

#### 3.1. Craze nucleation

During the simulations, the RVE is deformed at a constant linear strain rate of  $10^{-3} \text{ s}^{-1}$ , and the local stresses and strains are monitored meanwhile a hydrostatic stress-based craze-nucleation criterion is evaluated. This criterion identifies a critical hydrostatic stress of 40 MPa to be the onset of craze nucleation, provided that plastic deformation occurred in this zone [1]. For this purpose the softening parameter,  $D$  ( $D > 0$  indicates plastic deformation), and the hydrostatic stress,  $\sigma_h$ , are monitored. When a critical level of 40 MPa is exceeded, it is assumed that a void is nucleated and that the RVE suffered from macroscopic brittle fracture. Thus the actual details of craze formation, the craze-growth process and the final local failure are not incorporated, since they all are considered to be of secondary importance only.

#### 3.2. Incorporation of an absolute length-scale

Since the  $T_g$ -depression reported for thin, free-standing polystyrene films ( $< 100 \text{ nm}$ ) are rationalised by an enhanced segmental mobility of the chains near a free surface [34,35], a similar approach is used in our simulations. But instead of bringing the  $T_g$  of the material closer to ambient temperature, a temperature gradient, involving an increased temperature, in a thin layer near a free surface is introduced. The thermally enhanced mobility, by which this is accompanied, results in a lower modulus, yield stress and strain hardening and a reduced strain softening. One could argue that the nature of the enhanced mobility in thin films is not necessarily equal to (isotropic) thermally induced segmental mobility and that its influence on modulus, yield stress and strain hardening might differ. But we will remain to the experimentally determined values at the surface of isotropic bulk polystyrene [20].

To incorporate length-scale effects, a temperature profile is generated in the RVE, prescribing a temperature equal to the glass-transition temperature ( $105^\circ\text{C}$ ) is prescribed at internal free-surfaces, i.e. void edges. In a time-dependent

computation a natural temperature profile is generated. Since for thin free-standing films of less than 100 nm effects of  $T_g$ -depressions are reported [34,35], the distance over which the temperature profile is allowed to evolve is taken equal to 50 nm. This measure determines the absolute size of the RVE and the dimensions of the inclusions. From the diameter of the spheres and their volume fraction, a typical inter-particle distance can be derived which allows comparison of simulations and experiments.

The temperature profile obtained is used as thermal boundary condition in the subsequent simulations of the deformation. The evaluation of the craze-nucleation criterion is identical to that used in the isothermal simulations.

### 4. Results

#### 4.1. BDT induced by temperature

Fig. 2 shows the equivalent strain,  $\epsilon_{\text{eq}}^1$  at four different stages (macroscopic strains of 5, 10, 15 and 20%) during deformation of the RVE at  $20^\circ\text{C}$  (top) and  $80^\circ\text{C}$  (bottom). The heterogeneity of the structure first induces plastic deformation in the ligaments in between the voids which display yielding and strain softening (Fig. 2,  $20^\circ\text{C}$ , 5%).

The pronounced strain softening at  $20^\circ\text{C}$ , see, e.g. Ref. [20], results in a substantial load drop in the ligaments after yielding and, since the strain hardening of polystyrene is very weak, with ongoing deformation the ligaments are not able to transfer load to the surrounding material. The top row of figures illustrates the extreme localisation of strain in neighbouring ligaments (the dark colours in Fig. 2 represent the regions with the highest strain) that interconnect and form a localisation path. The excessively deformed ligaments surrounded by a hardly deformed matrix indicate that only a limited material volume participates in the deformation. Brittle fracture will occur either due to the early craze-initiation in between the voids, or by exceeding the maximum tensile strength within a ligament.

With increasing temperature, the yield stress and strain softening decrease significantly [20]. Although the force required to induce yielding in a ligament is consequently lower, the reduced drop in load after yielding is also low compared to the drop at  $20^\circ\text{C}$ , and can more easily be stabilised. The bottom row of Fig. 2, which shows the deformation at  $80^\circ\text{C}$ , illustrates this. At 5% of macroscopic strain the deformation is similar to that at  $20^\circ\text{C}$  and 5% strain. However, the strain in the ligaments is more easily stabilised and induces sequential yielding throughout the RVE. As a result a larger material volume participates in the deformation.

Fig. 3 shows the engineering stress versus the macroscopic draw ratio of the RVE. The apparent yield stress of

<sup>1</sup> The equivalent strain is defined as the scalar norm of the logarithmic strain tensor,  $\mathbf{E}$ , according to:  $\epsilon_{\text{eq}} = \sqrt{\frac{2}{3} \mathbf{E}^{\text{d}} : \mathbf{E}^{\text{d}}}$ .

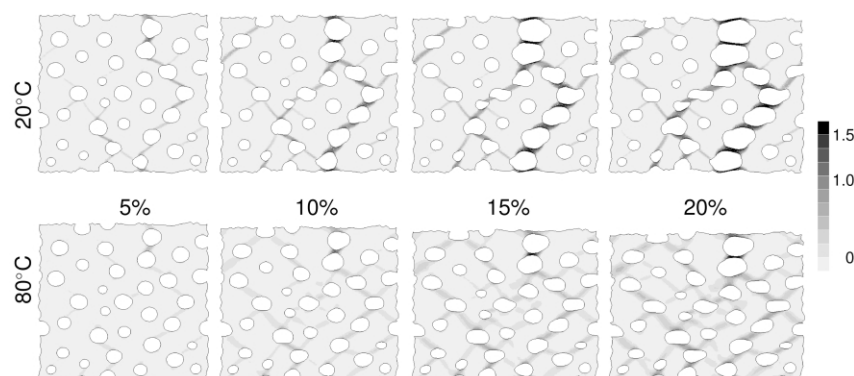


Fig. 2. Equivalent strain,  $\epsilon_{eq}$ , in the RVE in tension at 20 (top) and 80 °C (bottom).

the RVE is of course lower than for the homogeneous material due to the incorporation of voids. Similar to the homogeneous material, both yield stress and strain softening are significantly reduced by increasing the testing temperature.

Although localisation of strain and crazing are strongly related, this does not imply that crazing is inhibited if the strain is delocalised and that a transition from crazing to shear yielding is achieved at high temperatures. To evaluate the craze-nucleation criterion, the maximum hydrostatic stress is monitored in the plastically deformed regions. The simulations show that around the macroscopic yield point of the RVE, the hydrostatic stress reaches a maximum. Therefore in Fig. 4 the critical hydrostatic stress in the RVE is given at this stage (macroscopic strain of 2.5%). The black regions indicate the zones where a hydrostatic stress of 40 MPa is exceeded.

Until 60 °C the hydrostatic stress of 40 MPa is exceeded at low strains, although the number and size of the regions where it is exceeded decreases drastically with temperature. At all these temperatures the RVE is considered to suffer from macroscopic brittle fracture. For 80 °C at this stage the criterion is not exceeded. To judge whether at 80 °C a critical hydrostatic stress is never exceeded, the development of this stress during deformation is studied in more detail. Fig. 5 shows the maximum hydrostatic stress as function of macroscopic draw ratio at various temperatures.

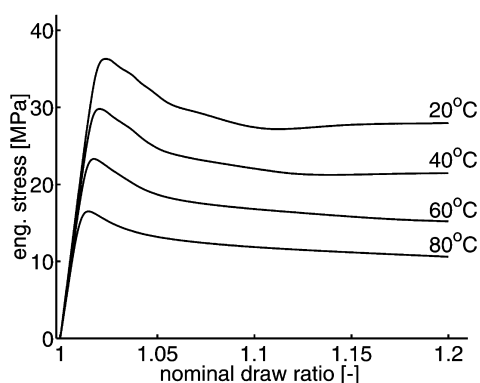


Fig. 3. Engineering stress versus nominal draw ratio of the RVE at various temperatures.

The dashed line indicates the critical hydrostatic stress level of 40 MPa, the onset of void nucleation. At 20 °C, this level is already exceeded at 1% macroscopic strain. Although the maximum hydrostatic stress levels decrease when the temperature is increased, at 40 and 60 °C the critical hydrostatic stress is still exceeded at a few percent of macroscopic strain. At 80 °C the maximum in  $\sigma_h$  remains under the critical stress level until far beyond the macroscopic yield point of the RVE and at 15% macroscopic strain a critical level is reached in one ligament only (see Fig. 5b). This ligament is cold-drawn up to strains exceeding 150% and hence will not very likely exhibit crazing anymore, similar to pre-oriented polystyrene [38]. Therefore, the conclusion is justified that at 80 °C no crazing is observed and hence ductile deformation behaviour is obtained in voided polystyrene with 20% voids.

To refine the temperature where the transition from crazing to shear yielding occurs, additional simulations were performed at 70 and 75 °C. At 70 °C the critical hydrostatic stress is reached at a few percent strain, whereas at 75 °C this occurs only at 10% macroscopic strain, in a ligament where the local strain exceeds 100%. Similar to the simulation at 80 °C, polystyrene is not likely to exhibit crazing anymore at 75 °C. From these simulations it can be concluded that in between 70 and 75 °C, crazing is inhibited during deformation and hence a temperature induced brittle-to-ductile transition is achieved for a heterogeneous polystyrene structure with 20% voids.

Since it was shown that yield stress and strain softening are key parameters in the developing level of hydrostatic stress, it is reasonable to assume that this BDT temperature is sensitive to the thermal history of the polymer and the strain rate of the test.

To validate the simulations, experiments were performed on polystyrene (PS N5000, Shell) filled with 20% core-shell rubbers (Kane Ace B511, 200 nm, Kaneka), which was mixed on a 25 mm Werner and Pfleiderer co-rotating twin-screw extruder, ZSK 25, at a temperature of 160 °C and a rotation speed of 152 rpm. The material flux was optimised for the highest torque in order to achieve proper particle dispersion. Next the blend was injection moulded into tensile bars, according to ISO 527. Before compounding, the



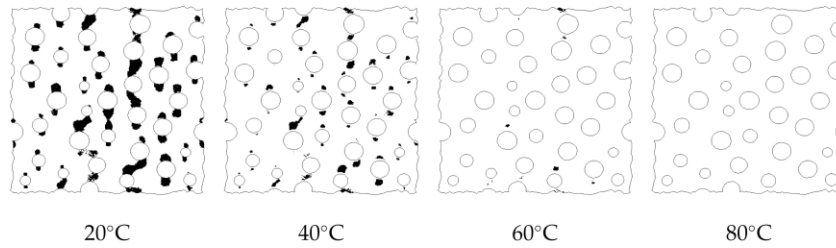


Fig. 4. Hydrostatic stress in the RVE around the macroscopic yield point (2.5% macroscopic strain): black regions indicate the regions in which after plastic deformation a critical hydrostatic stress level of 40 MPa is exceeded.

materials were dried in a vacuum-oven for 5 days. As was shown by TEM in a study on similar blends, compounded in an identical way, good dispersion of the core-shell rubbers is achieved under these processing conditions [28].

The injection moulded tensile bars were subjected to uni-axial tensile tests at conditions identical to those used in the simulations (temperatures ranging from 20 to 100 °C and a strain rate of  $10^{-3} \text{ s}^{-1}$ ). Fig. 6a shows the engineering stress versus the nominal draw ratio during a tensile test at 80 °C in both, experiments (circles) and simulations (solid line). They compare rather well. This suggests that the core-shell rubbers are non-adhering and that they hardly participate in the deformation process. Representing them as voids seems to be a valid assumption. The small discrepancies in yield stress can be rationalised by the difference in thermal history of the injection moulded tensile bars and compression moulded samples used for the characterisation of the material parameters of the model [20].

Fig. 6b shows that the experiments confirm the

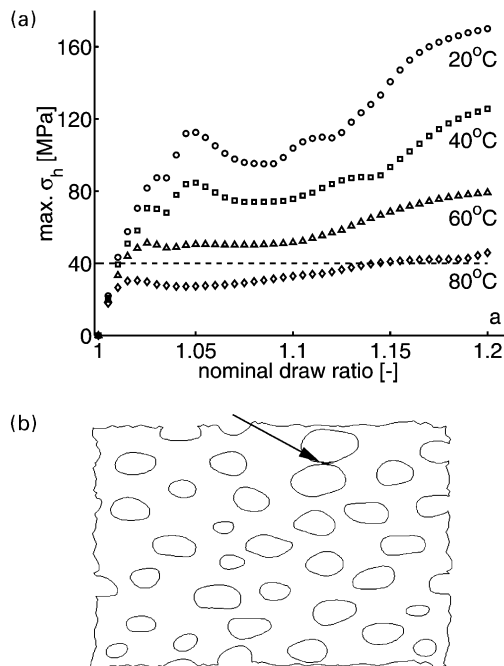


Fig. 5. Developing hydrostatic stress in RVE at various temperatures (a) and hydrostatic stress exceeded at highly deformed ligament, indicated by the arrow, at 80 °C.

observations in the simulations: at a temperature of around 70–75 °C a sharp transition from brittle-to-ductile is observed. The open circles with error-bars represent the macroscopic strains reached in the uni-axial tensile tests, which were around 100%, whereas the simulations were stopped at 20% macroscopic strain because of the necessity of remeshing within the ligaments. The arrows indicate that by remeshing also in the simulations larger strains could have been reached. The small discrepancies in strain at break in the region of 60–70 °C can be explained by the fact that in the simulations brittle fracture is assumed to occur at the first moment a critical hydrostatic stress of 40 MPa is exceeded, whereas experimentally failure at more sites is required for macroscopic failure. Hence the strain at break in brittle failure is always underestimated in the simulations.

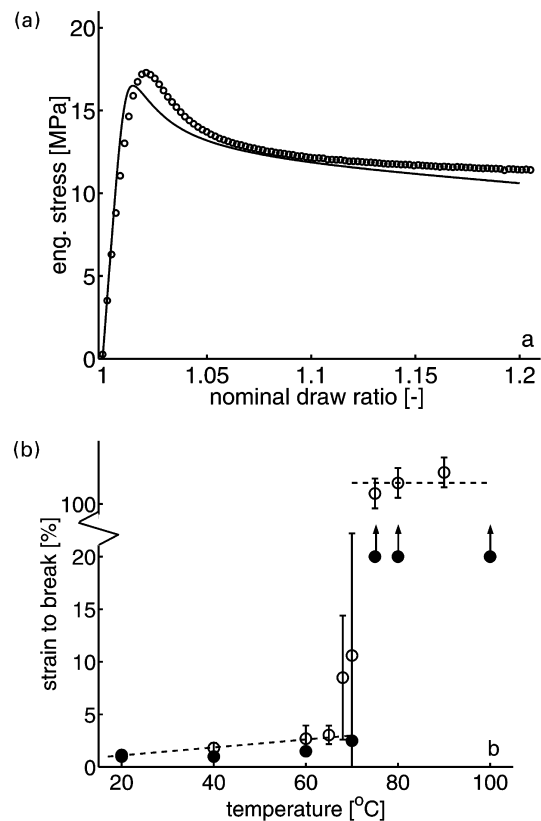


Fig. 6. Stress/strain curves at 80 °C (a), experiment (circles) and simulation (solid line), and temperature induced BDT (b), experiments (open circles) and simulations (filled circles). Arrows indicate that the simulations were stopped before failure was encountered.

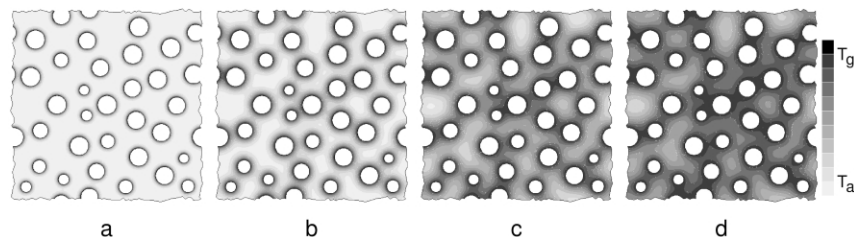


Fig. 7. Temperature at various stages in the thermal simulation, representing voided polystyrene with voids of 150, 80, 40, and 20 nm, respectively.

The macroscopic ductile fracture, which occurs at high strains (above 70 °C) in the experiments, is the result of sequential failure of the polymer ligaments when their tensile strength is exceeded.

#### 4.2. BDT induced by length-scale effects

The presence of an absolute length-scale in amorphous polymer is modelled by a temperature gradient over a thin layer near a free surface. In Fig. 7 the temperature profiles are given at various moments in time during the simulation. The grey value-bar on the right-hand side of the figure indicates that the temperature on the free surface (dark colour) is equal to the bulk glass-transition ( $T_g$ , 105 °C), whereas in the bulk the temperature remains equal to the ambient temperature ( $T_a$ , 20 °C).

In Fig. 7a the increase in temperature has evolved to approximately one third of the diameter of the sphere. Assuming that the influence of the free surfaces around the voids runs 50 nm deep, this RVE represents a polystyrene matrix with 20% inclusions of 150 nm in diameter. Following this procedure, the sizes of the inclusions of Fig. 7b–d are estimated to be, respectively 80, 40 and 20 nm.

The temperature distributions, fixed after being interrupted on their development, are used as boundary conditions for the coupled simulation, where the deformation is determined. In Fig. 8 the results are given for the deformation of an RVE in which the absolute length-scale has no influence (diameter voids equals 1  $\mu\text{m}$ , top) and one where it has (40 nm inclusions, bottom). For the large voids, the deformation equals that of the simulation as presented

before at a temperature of 20 °C, see Fig. 2: a strong localisation of strain in the thin ligaments in between the voids. For the 40 nm inclusions, Fig. 8 (bottom), the temperature gradient results in a reduction in yield stress and strain softening in a thin layer around the inclusions. This leads to a slightly less localised deformation although strain still tends to localise within a few ligaments.

The stress strain curves for the RVE with different sizes of inclusions, given in Fig. 9, show that, with decreasing inclusion size and hence decreasing ligament thickness in between the particles, the yield stress and the strain softening of the RVE strongly decrease.

To evaluate whether these materials exhibit crazing, the hydrostatic stress has to be evaluated again during the simulations. In Fig. 9 the maximum hydrostatic stress is presented as function of the macroscopic draw ratio of the RVE for four different sizes of inclusions. For the larger spheres, 1  $\mu\text{m}$  and 80 nm the critical hydrostatic stress is already exceeded at a macroscopic strain of 1–2%. For the 40 nm spheres, the hydrostatic stress remains under a critical value far beyond the macroscopic yield point of the RVE. At macroscopic strains of 10% a critical stress level is reached somewhere within a strongly deformed ligament. Since the local strain in this ligament exceeds 100%, is not likely to craze anymore and therefore it seems reasonable to assume that at these small inclusion-sizes crazing is inhibited and shear yielding occurs throughout the specimen. Again the macroscopic strain is limited to 20% for computational reasons (Fig. 10).

All simulations are summarised in Fig. 11 where the strain at break is represented as function of the inter-particle distance (ID), which can be derived from the expression

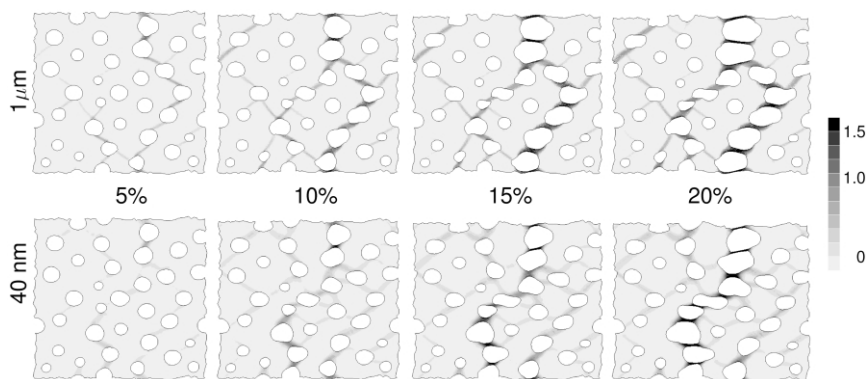


Fig. 8. Equivalent strain,  $\epsilon_{eq}$ , in the RVE in tension for inclusions of 1  $\mu\text{m}$  (top) and 40 nm (bottom).

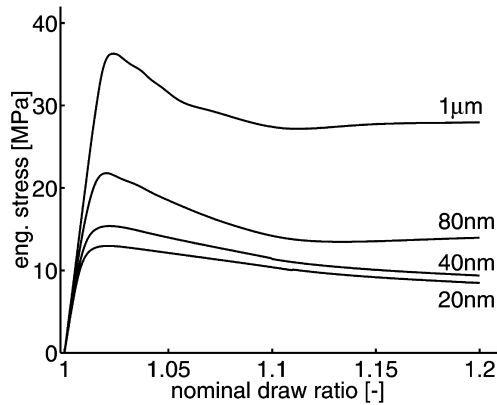


Fig. 9. Engineering stress versus nominal draw ratio for voided PS (20% voids) and inclusion sizes of 1  $\mu\text{m}$ , 80, 40 and 20 nm.

[31]:

$$ID = D \left[ \left( \frac{\alpha \pi}{6V_f} \right)^{1/3} - 1 \right]$$

where  $D$  is the diameter and  $V_f$  the volume fraction of the inclusions. In this equation  $\alpha$  accounts for the stacking of the rubber spheres within the matrix. Wu [31] showed that for nylon–rubber blends the packing resembles a simple cubic lattice for the lower volume fractions ( $V_f < 40\%$ ), and  $\alpha$  equals 1.

At larger void sizes and thus large IDs crazing is observed in the numerical simulations and only at a void diameter smaller than 40 nm crazing is inhibited. Since the volume fraction of the inclusions equals 20%, at a ID of approximately 15 nm, a sharp increase in strain to break is observed, indicating that a transition from crazing to shear yielding is achieved. The arrows once again indicate that the simulations were stopped for numerical reasons before failure occurred.

Experimental results provided by Van der Sanden [28] and Jansen [30] showed that a BDT occurs in non-adhering core-shell rubber filled polystyrene at 55 vol.% inclusions of 200 nm and 35 vol.% inclusions of 80 nm, respectively. In Jansen's example a critical inter-particle distance of 11.5 nm is found. Van der Sanden argued that high volume

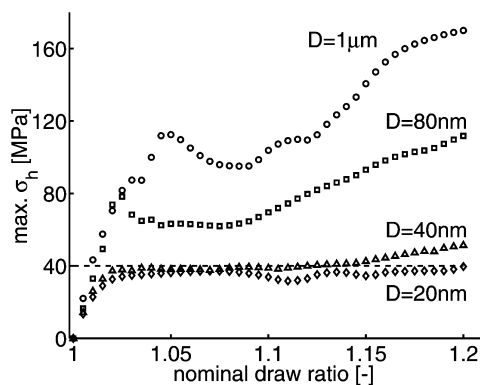


Fig. 10. The developing maximum hydrostatic stress versus nominal draw ratio in the plastically deformed zones of the RVE for various void-sizes.

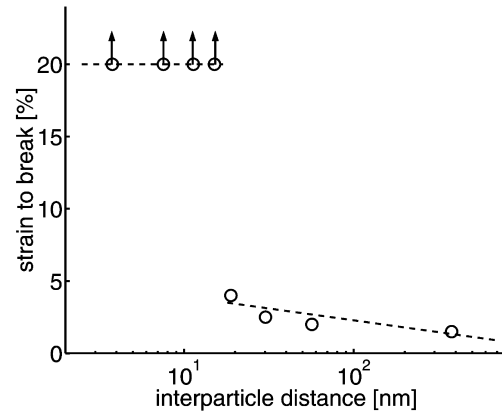


Fig. 11. Brittle-to-ductile transition induced by an absolute length-scale: ductile deformation behaviour at ID < 15 nm, arrows indicate the simulations were stopped before failure occurred.

fractions of rubber particles result in a face-centred cubic stacking and that  $\alpha$  is equal to 2. The associated critical inter-particle distance equals, therefore, 15 nm. These values compare well with the value found from the simulations.

The simulations, which are presented here, indicate the mobility of the polymer ligaments within the blends is strongly enhanced by increasing the amount of internal free surfaces.

## 5. Discussion and conclusions

In this paper numerical simulations of the deformation of voided polystyrene were performed to investigate the capability of finite element simulations, employing the compressible Leonov model, to predict brittle-to-ductile transitions in polystyrene.

In previous studies [20,39], it was shown that the post-yield behaviour plays a crucial role in the deformation of glassy polymers. Improvements must be focused on avoiding severe localisation of strain by eliminating strain softening and enhancing the strain hardening contribution of the polymer network. However, besides strain localisation, crazing will occur, which involves void nucleation in local plastically deformed zones under dilative stresses. Therefore, the control of build-up of hydrostatic stresses is important as well.

It is generally accepted that only by creating a heterogeneous structure, the hydrostatic stresses can be relieved and toughness improved. In rubber-modified polystyrene (HIPS) improved properties can be attributed to a deformation mechanism of multiple crazing and not to a transition from crazing to shear yielding. Consequently room for further improvement remains.

Finite element simulations of voided polystyrene were performed at a strain rate of  $10^{-3} \text{ s}^{-1}$  at various temperatures. During the simulations a craze-nucleation criterion (a critical hydrostatic stress of 40 MPa, preceded by plastic

deformation) was evaluated to determine whether crazing would occur. It was demonstrated that a brittle-to-ductile transition could be achieved by raising the testing temperature to around 75 °C. At this temperature the critical hydrostatic stress is not exceeded. The results of the numerical simulations are in good agreement with the experimental results, using tensile tests on filled polystyrene (20% non-adhering core-shell rubber of 200 nm), which exhibited a brittle-to-ductile transition at a temperature around 70 °C.

Reducing the ligament thickness in the voided structure is another, from application point of view far more interesting, route to achieve a brittle-to-ductile transition. The absolute length-scale encountered here is deduced from the measured  $T_g$  depression in thin, freestanding polystyrene films, and attributed to an enhanced mobility of polymer chains near a free surface. The enhanced mobility was accounted for in the simulations by assuming a temperature gradient from the free surface into the bulk. The depth of this temperature gradient determines the absolute length-scale of the material. The simulations demonstrate that, by decreasing the absolute length-scale exceeding of the critical hydrostatic stress level can be avoided and a transition from crazing to shear yielding can be achieved. At 20% voids of 40 nm in diameter, representing an inter-particle distance of approximately 15 nm, a brittle-to-ductile transition is observed, which correlates well with experimental observations of highly filled polystyrene/non-adhering rubber blends [28–30]. The approach followed here implies that the critical inter-particle distance is dependent on both temperature and strain rate.

The simulations, which are presented in the last section, indicate the mobility of the polymer ligaments within the blends is strongly enhanced by increasing the amount of internal free surfaces. As is shown in Fig. 9 this leads to a significant drop in modulus and yield stress and has a similar effect on the mechanical properties as the application plasticisers. For an engineering material, however, a less pronounced decrease in modulus and yield stress would be desirable.

Although at smaller inter-particle distances the maximum hydrostatic stress is sufficiently reduced to inhibit crazing, the localisation of strain within the ligaments is still quite severe, see Fig. 8 (bottom). The incorporation of *pre-cavitated*, adhering core-shell rubbers, as proposed by Refs. [17,30], could support these ligaments during deformation to transfer more load. As a result they would be able to induce sequential yielding throughout the RVE, increase the material volume participating in the deformation and hence further improve the toughness.

## Acknowledgements

The authors wish to acknowledge the financial support provided by the Dutch Technology Foundation (STW)

(Grant EWT.3766), and J.T.A. Kierkels for his assistance in the experimental work.

## References

- [1] van Melick HGH, Bressers OFTJ, den Toonder JMJ, Govaert LE, Meijer HEH. A micro-indentation method as a probe for the craze-initiation stress in glassy polymers. *Polymer* 2002, accepted.
- [2] Haward RN, Thackray G. *Proc R Soc Lond A* 1967;302:453–572.
- [3] Boyce MC, Parks DM, Argon AS. *Mech Mater* 1998;7:15–33.
- [4] Hasan OA, Boyce MC, Li XS, Berko S. *J Polym Sci, Part B: Polym Phys* 1993;31(2):185–97.
- [5] Arruda EM, Boyce MC. *Int J Plast* 1993;9(6):697–720.
- [6] Boyce MC, Arruda EM, Jayachandran R. *Polym Engng Sci* 1994;34(9):716–25.
- [7] Wu PD, van der Giessen E. *J Mech Phys Solids* 1993;41(3):427–56.
- [8] Wu PD, van der Giessen E. *Int J Plast* 1995;11(3):211–35.
- [9] Govaert LE, Timmermans PHM, Brekelmans WAM. *J Engng Mater Technol* 2000;122(2):177–85.
- [10] Tervoort TA, Smit RJM, Brekelmans WAM, Govaert LE. *Mech Time-dependent Mater* 1998;1(3):269–91.
- [11] Tervoort TA, Govaert LE. *J Rheol* 2000;44(6):1263–77.
- [12] Tervoort TA, Klompen ETJ, Govaert LE. *J Rheol* 1996;40(5):779–97.
- [13] Smit RJM, Brekelmans WAM, Meijer HEH. *Comput Meth Appl Mech Engng* 1998;155(1–2):181–92.
- [14] Smit RJM, Brekelmans WAM, Meijer HEH. *J Mech Phys Solids* 1999;47(2):201–21.
- [15] Smit RJM, Brekelmans WAM, Meijer HEH. *J Mater Sci* 2000;35(11):2855–67.
- [16] Smit RJM, Brekelmans WAM, Meijer HEH. *J Mater Sci* 2000;35(11):2869–79.
- [17] Smit RJM, Brekelmans WAM, Meijer HEH. *J Mater Sci* 2000;35(11):2881–92.
- [18] Donald AM, Kramer EJ. *Polymer* 1982;23(3):457–60.
- [19] Donald AM, Kramer EJ, Bubeck RA. *J Polym Sci, Polym Phys Ed* 1982;20(7):1129–41.
- [20] van Melick HGH, Govaert LE, Meijer HEH. Localisation phenomena in glassy polymers: influence of thermal and mechanical history. *Polymer* 2002, submitted for publication.
- [21] Kramer EJ. Microscopic and molecular fundamentals of crazing. In: Kausch HH, editor. *Advances in polymer science* 52/53. Crazing in polymers, Berlin: Springer; 1983. p. 1–56.
- [22] Kramer EJ, Berger LL. Craze growth and fracture. In: Kausch HH, editor. *Advances in polymer science* 91/92. Crazing in polymers, vol. 2. Berlin: Springer; 1990. p. 1–68.
- [23] Donald AM, Kramer EJ. *J Mater Sci* 1982;17(7):1871–9.
- [24] Wu S. *Polym Engng Sci* 1990;30(13):753–61.
- [25] Bucknall CB. In: Haward RN, Young RJ, editors. *The physics of glassy polymers*, 2nd ed. London: Chapman & Hall; 1997. p. 363–412.
- [26] Bucknall CB, Smith RR. *Polymer* 1965;6:437.
- [27] Donald AM, Kramer EJ. *J Mater Sci* 1982;17(8):2351–8.
- [28] van der Sanden MCM, de Kok JMM, Meijer HEH. *Polymer* 1994;35:2995–3004.
- [29] Magalhaes AML, Borggreve RJM. *Macromolecules* 1995;28(17):5841–51.
- [30] Jansen BJP, Rastogi S, Meijer HEH, Lemstra PJ. *Macromolecules* 2001;34:3998–4006.
- [31] Wu S. *J Appl Polym Sci* 1988;35(2):549–61.
- [32] van der Sanden MCM, Meijer HEH, Lemstra PJ. *Polymer* 1993;34:2148–54.



- [33] Keddie JL, Jones RAL, Cory RA. *Eur Phys Lett* 1994;27(1):59–64.
- [34] Forrest JA, Mattsson J. *Phys Rev E* 2000;61(1):R53–6.
- [35] Forrest JA, Jones RAL. In: Karim A, Kumar S, editors. *Polymer surfaces, interfaces, and thin films*. Singapore: World Scientific; 2000. p. 251–94.
- [36] van Melick HGH, van Dijken AR, den Toonder MJM, Govaert LE, Meijer HEH. *Philos Mag A* 2002;82(10):2093–102.
- [37] van der Aa MAH, Schreurs PJG, Baaijens FPT. *Mech Mater* 2001;33: 555–72.
- [38] Ender DH, Andrews RD. *Polym Lett* 1965;36:3057–62.
- [39] Meijer HEH, Govaert LE, Smit RJM. A multi-level finite element method for modeling rubber-toughened amorphous polymers. In: Pearson R, editor. *Toughening of plastics*. Boston: American Chemical Society; 2000. p. 50–70.